İstanbul Journal of Pharmacy
Istanbul J Pharm2024, 54 (3): 456–465
DOI: 10.26650/IstanbulJPharm.2024.1449135

Original Article

Synthesis, characterization, and crystal structure of a novel spirocyclic 2-indolinone bearing a 5-(trifluoromethyl)benzothiazoline moiety

Asu Busra Temizer[1,2], Filiz Betül Kaynak[3], Nilgun Karalı[4]

[1]İstanbul University-Cerrahpaşa, Faculty of Pharmacy, Department of Pharmaceutical Chemistry, İstanbul, Türkiye
[2]İstanbul University, Institute of Graduate Studies in Health Sciences, Department of Pharmaceutical Chemistry, İstanbul, Türkiye
[3]Hacettepe University, Faculty of Engineering, Department of Physical Engineering, Ankara, Türkiye
[4]İstanbul University, Faculty of Pharmacy, Department of Pharmaceutical Chemistry, İstanbul, Türkiye

ABSTRACT

Background and Aims: Spirocyclic 2-indolinones are important and promising compounds because of their various biological activities in drug development studies. The main aim of this study is to determine spirocyclic, molecular and stereoisomeric structure of the new 5'-chloro-1',7'-dimethyl-5-(trifluoromethyl)-3*H*-spiro[1,3-benzothiazole-2,3'-indole]-2'-one (**4**) and to examine the contribution of the trifluoromethyl group.

Methods: Compound **4** was synthesized from the reaction of 2-amino-4-(trifluoromethyl)benzenethiol with 5-chloro-1,7-dimethyl-1*H*-indole-2,3-dione in ethanol. The purity and structure determination of compound **4** was carried out by elemental and spectral analyzes. The crystal structure of compound **4** was characterized by X-ray single crystal diffraction analysis method (SC-XRD). Additionally, compliance with Lipinski's rule of 5 (RO5) and some pharmacokinetic parameters of compound **4** were evaluated using the Qikprop modüle (Schrödinger).

Results: The molecular structure of **4** was confirmed by elemental and spectral (IR, ^{1}H NMR, ^{13}C NMR-APT, HSQC-2D, HMBC-2D and LCMS-APCI) data. The crystal, spirocyclic and stereoisomeric structure of compound **4** was elucidated by SC-XRD, and it was observed that N-H···O hydrogen bonding interactions take place within the molecular layers aligned parallel to the (010) plane. As a drug candidate, compound **4** exhibited physicochemical parameters consistent with Lipinski's RO5.

Conclusion: In the crystal, both intra- and intermolecular hydrogen bonds are present. The molecular packing is stabilized by intermolecular N— H···O hydrogen bonds.

Keywords: 2-Indolinone, Benzothiazoline, Crystal structure, Structural characterization, Synthesis.

INTRODUCTION

For pharmaceutical chemists, knowing the 3D structures of synthesized molecules are critical for obtaining and developing effective and safe drugs in the drug discovery and design process. Due to the interesting structure of spiro compounds and their importance in biological activity, there are many studies in the literature for the discovery of their 3D structures (Ding, Meazza, Guo, Yang & Rios, 2018). Spirocyclic compounds were first recognised in organic chemistry in the late 1800s and early 1900s and represent polycyclic structures in which one or more carbon atoms are common members of two or more different rings (Baeyer, 1900; Bariwal, Voskressensky & Van der Eycken, 2018). It is thought that polycyclic rings may pose compatibility problems and the presence of quaternary and generally chiral spiro atoms pose difficulties in terms of synthesising these compounds and determining their 3D structures.

Spirocyclic 2-indolinones derived from the 1*H*-indole-2,3-dione form polycyclic structures with relatively few compatibility problems. In particular, the presence of different heterocyclic rings fused at the position 3- of the 2-indolinone ring in bio-promicing natural products (the compounds **1-4**; Figure 1) has made spirocyclic 2-indolinone promising for drug discovery. Synthetic analogues of spirocyclic 2-indolinones have a broad therapeutic potential as antioxidants (Ermut, Karalı, Özsoy & Can, 2014 ; Karalı, Güzel, Özsoy, Özbey & Salman, 2010), antiviral (Jiang et al., 2006), anticancer (Altowyan et al., 2022; Abdelmouna et al., 2023) antimalarial (Schwertz et al., 2018; Rottmann et al., 2010), antimicrobial (Akdemir & Ermut, 2013), antidiabetic (Murugan, Anbazhagan & Narayanan,

Corresponding Author: Asu Busra Temizer **E-mail:** temizerab@gmail.com
Submitted: 08.03.2024 • **Revision Requested:** 21.07.2024 • **Last Revision Received:** 02.08.2024 • **Accepted:** 22.10.2024

2009) and potent nonpeptide inhibitors of p53-MDM2 interaction (Shangary et al., 2008; Zhao et al., 2013) (the compounds **5-7**; Figure 1).

Reactions of 1*H*-indole-2,3-diones with 1,2-disubstituted benzene derivatives have been attempted using different catalysts in different solvents to synthesize these important heterocyclic compounds (Dowlatabadi et al., 2011; Jain, Sharma & Kumar, 2012; Popp, 1969). Data in the literature have shown that different compounds are obtained from the reaction of 1*H*-indole-2,3-diones with 2-aminobenzenethiol, depending on the substitution at the position 1- of 1*H*-indole-2,3-dione. It has been noted that when at the position 1- of 1*H*-indole-2,3-dione is unsubstituted, spirobenzothiazine, indolobenzothiazine and benzothiazinone are obtained, while only the spirocyclic compound is synthesized from the reaction of *N*-methyl-1*H*-indole-2,3-dione (Dandia, Khanna & Joshi, 1990; Joshi, Dandia & Khanna, 1990). In later studies, a single spirobenzothiazole compound was sythesized by the reaction of 1*H*-indole-2,3-dione with 2-aminobenzenethiol in ethanol (Alam & Nawwar, 2002; Karalı et al., 2010; Ermut et al., 2014). In addition, these findings were confirmed by single-crystal X-ray diffraction analyzes of the spirocyclic compounds synthesized from 1*H*-indole-2,3-dione and *N*-methyl-1*H*-indole-2,3-dione derivatives (Figure 2) (Karalı et al., 2010; Akkurt, Karaca, Ermut, Karalı & Büyükgüngör, 2010).

Considering these findings, we synthesized a novel spirocyclic 5-chloro-1,7-dimethyl-2-indolinone bearing a 5-(trifluoromethyl)benzothiazoline moiety and, characterized the crystal and spirocyclic structure of the compound by spectral and single crystal X-ray diffraction analyzes. Moreover, compliance with Lipinski's rule of 5 (RO5) and the ADME criteria was evaluated *in silico* using the Qikprop module. Unlike planar aromatic compounds, non-planar and especially rigid spiro heterocyclic systems exhibit stronger affinity for the three-dimensional regions of proteins that function as biological targets. In our current study, the spirooxindole derivative compound we synthesized is ideal candidate for various biological activities, including antiviral, antioxidant, and anticancer effects. In this context, comparisons with previous studies and similar molecules will be made to demonstrate the significant contribution of this compound.

MATERIALS AND METHODS

Chemistry

2-Amino-4-(trifluoromethyl)benzenethiol and methyliodide are purchased Sigma-Aldrich Chemical Co. (St. Louis, MO). 5-Chloro-7-methyl-1*H*-indole-2,3-dione is purchased Abcr. Devices used in analysis; IR spectra were determined on KBr discs using a Shimadzu IR Affinity-1 FTIR spectrophotometer. Elemental analysis was conducted on a Thermo Finnigan Flash EA 1112 elemental analyzer. ^{1}H NMR, ^{13}C NMR-APT, HSQC-2D and HMBC-2D spectra were obtained on a Bruker Avance III HD (600 MHz). The mass spectrum was confirmed on Agilent Infinity 1260 II LC-MS. The melting points were measured on the Büchi Melting Point B-540 and Büchi Melting Point M-560 instruments.

Synthesis of 1,7-dimethyl-5-chloro-1*H*-indole-2,3-dione (2)

A mixture of 5-chloro-7-methyl-1*H*-indole-2,3-dione (1) (5 mmol) and 0.97 g anhydrous K_2CO_3 (7 mmol) in 10 mL DMF was stirred at room temperature for 1 h. Methyliodide (15 mmol) and 0.17 g KI (1 mmol) as catalyst were added to the mixture and heated at 50-60ºC with refluxing and stirring continuously until the reaction was complete. The mixture was first evaporated to dryness at reduced pressure to give the crude product, then the solid product obtained was washed with water to remove excess K_2CO_3 and KI and purified by crystallisation with ethanol.

Brown powder (yield 91%), M.p.: 171-173 °C. **IR** (KBr) ν max (cm^{-1}): 3064, 3043 (aromatic C-H), 2951, 2889 (aliphatic C-H), 1737, 1687 (C=O), 1616, 1489, 1473 (C=C). **^{1}H NMR** (DMSO-d_6, 600 MHz) δ (ppm): 2.53 (s, 3H, ind. C_7-CH_3), 3.39 (s, 3H, ind. N-CH_3), 7.42 (d, J = 2.3 Hz, 1H, ind. C_6-H), 7.55 (d, J = 2.5 Hz, 1H, ind. C_4-H); **^{13}C NMR-APT** (DMSO-d_6, 126 MHz) δ (ppm): 18.35 (ind. C_7-CH_3), 29.61 (ind. N-CH_3), 119.93 (ind. C_{3a}), 122.05 (ind. C_4), 125.00 (ind. C_7), 127.61 (ind. C_5), 140.50 (ind. C_6), 148.23 (ind. C_{7a}), 159.22 (ind. C_3), 183.20 (ind. C_2).

Synthesis of 5'-chloro-1',7'-dimethyl-5-(trifluoromethyl)-3*H*-spiro[1,3-benzothiazole-2,3'-indol]-2'-on (4)

To a solution of 5-chloro-7-methyl-1*H*-indole-2,3-dione (2) (2.5 mmol) in absolute ethanol (20 mL) was added 2-amino-4-(trifluoromethyl)benzenethiol (3) (2.5 mmol). The mixture was heated in a water bath under a reversing cooler until the reaction was terminated. The product formed was separated by filtration and purified by crystallization from an ethanol- water mixture (Karalı et al., 2010).

Yellow powder (yield 77%), M.p.: 236-238 °C; **IR** (KBr) ν max (cm^{-1}): 3337 (N-H), 3064, 3044 (aromatic C-H), 2936, 2870 (aliphatic C-H), 1705 (C=O) 1599, 1581, 1458 (C=C); **^{1}H NMR** (DMSO-d_6, 600 MHz) δ (ppm): 2.55 (s, 3H, ind. C_7-CH_3), 3.39 (s, 3H, ind. N-CH_3), 6.77 (d, J = 1.8 Hz, 1H, b.t. C_4-H), 6.98 (dd, J = 8.0, 1.8 Hz, 1H, b.t. C_6-H), 7.28 (d, J = 8 Hz, b.t. C_7-H), 7.29 (d, J = 2.2 Hz, 1H, ind. C_6-H), 7.50 (d, J = 2.2 Hz, 1H, ind. C_4-H), 7.69 (s, 1H, b.t. N-H); **^{13}C NMR-APT** (126 MHz, DMSO-d_6) δ (ppm): 18.44 (ind. C_7-CH_3), 29.81 (ind. N-CH_3), 74.48 (spiro C), 104.21 (q, J= 3.6 Hz, b.t. C_4), 116.01 (q, J= 4.1 Hz, b.t. C_6), 121.88 (b.t. C_7), 123.42 (ind. C_7), 123.58 (ind. C_4), 124.94 (q, J= 272.2 Hz, CF_3), 127.22 (q, J= 31.4 Hz, b.t. C_5), 127.33 (ind. C_5), 129.98 (b.t. C_{7a}), 131.90

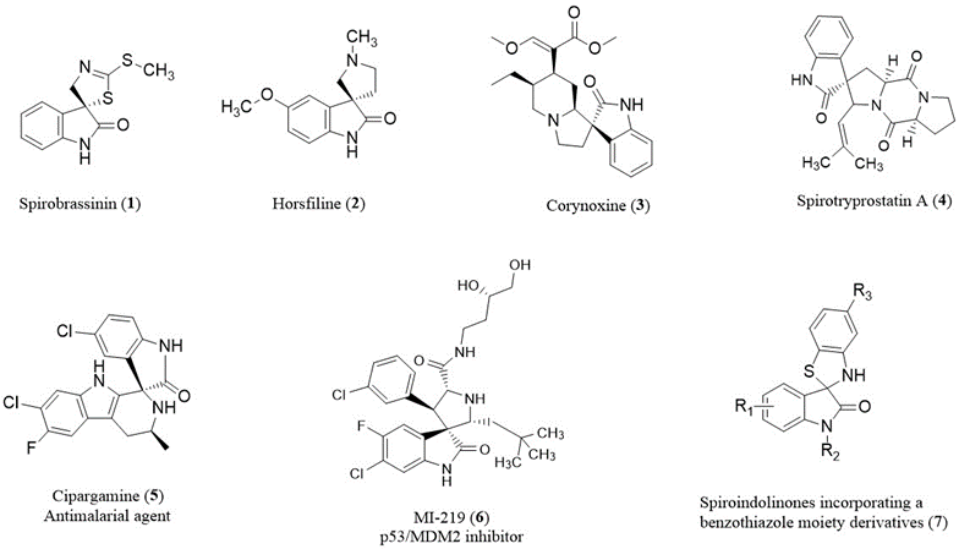

Figure 1. Chemical structures of spirocyclic 2-indolinone derivatives.

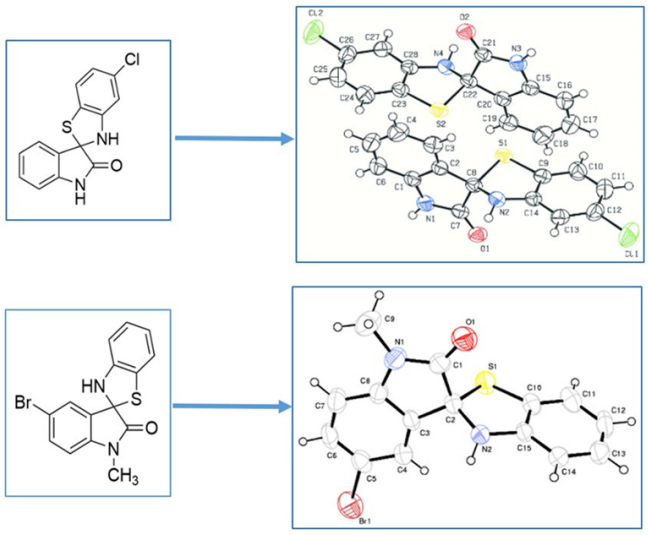

Figure 2. Spirocyclic 2-indolinone derivatives with confirmed crystal structures.

(ind. C_{3a}) , 134.00 (ind. C_6), 139.93 (ind. C_{7a}), 147.94 (b.t. C_{3a}), 175.02 (ind. C_2). **LC-MS (ESI)**: 407.0, 409.0 ([M+Na]$^+$; 100, 38), 385.0, 387.0 ([M+H]$^+$, 38, 13); **Analyses (%) cald for $C_{17}H_{12}ClF_3N_2OS$:** C, 53.06; H, 3.14; N, 7.28; S, 8.33. Found: C, 52.83; H, 3.11; N, 7.43; S, 8.27.

X-Ray Crystal Structure Determination and Refinement

The single-crystal X-ray data were collected on a STOE IPDS II image plate diffractometer at 293 K. Graphite-monochromated MoKα radiation (λ = 0.71073 Å) and the w-scan technique were used. Compound **4** was solved by direct methods using SHELXS-97 (Sheldrick, 1997) and refined through the full-matrix least-squares method using SHELXL-2014 (Sheldrick, 2015), implemented in the WinGX (Farrugia, 1999) programme suite. The non-hydrogen atoms were refined with the anisotropic displacement parameters.

Data collection and cell refinement were carried out using Stoe X-AREA (Stoe & Cie, 2002), while data reduction was conducted using Stoe X-RED (Stoe & Cie, 2002). The general-purpose crystallographic tool PLATON (Spek, 2009) was used for the structure analysis and presentation of the results. The dihedral angles were calculated using the PARST95 programme (Nardelli, 1995).

The hydrogen atom attached to the N2 atom was located using a difference Fourier map, and its coordinates and atomic displacement parameters were refined isotropically (N2-H2 = 0.81(2) Å). All remaining hydrogen atoms were placed geometrically, with C-H distances ranging from 0.93 to 0.97 Å, and Uiso(H) values set to 1.5 Ueq(C) for methyl hydrogen atoms and 1.2 Ueq(C) for other hydrogen atoms.

In silico analyses

Compliance with Lipinski's RO5 and some pharmacokinetic parameters of compound **4** were analysed *in silico* using the Qikprop module in Schrödinger (QikProp, Schrödinger, LLC, New York, NY 2018).

RESULTS AND DISCUSSION

Chemistry

5-Chloro-1,7-dimethyl-1*H*-indole-2,3-dione (**2**) was synthesized by methylation from the position 1- of indole ring with CH_3I of 5-chloro-7-methyl-1*H*-indole-2,3-

dione (**1**) using K_2CO_3 and KI as catalysts in DMF medium. New 5'-chloro-1',7'-dimethyl-5-(trifluoromethyl)-3*H*-spiro[1,3-benzothiazole-2,3'-indol]-2'-one (**4**) was obtained by the reaction of 5-chloro-1,7-dimethyl-1*H*-indole-2,3-dione (**2**) with 2-amino-4-(trifluoromethyl)benzenethiol (**3**) (Figure 3). The structure of the synthesized compound **4** was confirmed by spectral (IR, ^{1}H NMR, ^{13}C NMR-APT, HSQC-2D, HMBC-2D, and LC-MS) and analytical data.

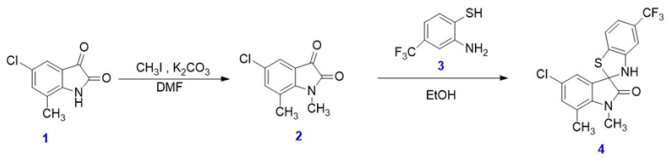

Figure 3. Synthesis of compound **4**.

Although the lactam group does not exhibit a strong nucleophilic character, it has the ability to undergo nucleophilic reactions in the enol form because of its weak acidic properties. K_2CO_3 used as a catalyst separates the proton of lactam and converts 5-chloro-7-methyl-1*H*-indole-2,3-dione (**1**) into the enol form. The anilide nitrogen of isatin, which is nucleophilic, attacks the carbon atom of iodomethane, forming an electrophilic centre. Because of this attack, a new bond is formed between the methyl carbon and the anilide nitrogen atoms and the iodide is separated to give 5-chlorine-1,7-dimethyl-1*H*-indole-2,3-dione (**2**). The condensation reaction between the amino group at the 2-amino-4-(trifluoromethyl)benzenethiol (**3**) and the ketone carbonyl of 5-chloro-1,7-dimethyl-1*H*-indole-2,3-dione (**2**) starts with the nucleophilic attack. In the intermediate product formed, (-) charged alkoxide group attacks the (+) charged amino group. This leads to the formation of the intermediate 3-hydroxy-3-anilino-5-chloro-1,7-dimethyl-1,3-dihydro-2*H*-indol-2-one, and by the elimination of a water molecule, 3-phenylimino-5-chloro-1,7-dimethyl-1,3-dihydro-2*H*-indol-2-one is formed. The 4-(trifluoromethyl)-benzenethiol sulfhydryl group attacks the imine carbon to form a new bond between the sulphur and carbon atoms. The (+) charged thioether group at the spirobenzothiazoline intermediate is neutralized by attracting electrons towards itself, while (-) charged secondary amine attacks the thioether proton. As a result of this reaction, compound **4** was obtained (Figure 4) (Dandia et al., 2006).

In the IR spectrum of compound **2**, ketone and lactam C=O stretching bands were observed at 1737 and 1687 cm^{-1}, respectively. The spectrum of compound **4** showed absorption bands at 3337 and 1705 cm^{-1} resulting from the benzothiazoline NH and lactam C=O functions, respectively, and the ketone C=O band was not observed (Allam & Nawwar, 2002; Castineiras, Gómez & Sevillano, 2000). The benzothiazoline NH proton signal was observed as a singlet at δ 7.69 ppm in the ^{1}H NMR spectrum of compound **4**. The benzothiazoline C_4 and C_6 proton signals due to the more shielding effect of the amine group on the protons at the positions *o*- and *p*- of the phenyl

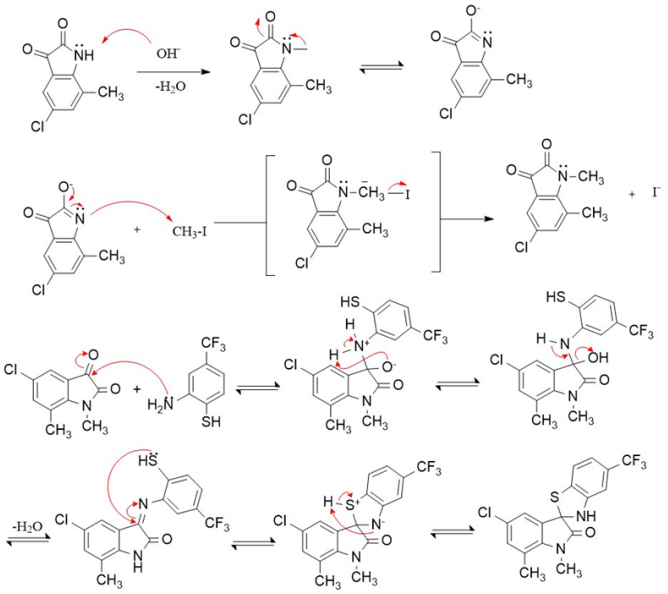

Figure 4. Possible synthesis mechanism of compound 4.

ring were determined at δ 6.77 (doublet, *m*-pairing) and 6.98 (doublet doublet, *o*- and *m*- pairings) ppm, respectively. The benzothiazoline C_7 proton resonated more downfield than the benzothiazoline C_4 and C_6 protons as a result of the deshielding effect of the thioether and trifluoromethyl groups and signaled as a doublet (*o*-pairing) at δ 7.28 ppm. The chemical shift values of the phenyl protons of 3-(trifluoromethyl)aniline (SDBS 3865) and the values calculated with the shift parameters of sulphur and amine groups confirmed the chemical shift values of the detected benzothiazoline ring protons and the substituent effects (Laatsch, Thomson & Cox, 1984; Santes, Rojas-Lima, Santillan & Farfàn, 1999; Ermut et al., 2014). In the spectrum of compound **2**, the indole C_4 and C_6 protons were observed as doublets (*m*- pairing) at δ 7.55 and 7.42 ppm, respectively. Whereas, in the spectra of compound **4**, indole C_4 and C_6 protons were shown as doublets (*m*- pairing) at δ 7.50 and 7.29 ppm, respectively. Methyl protons at positions 1- and 7- of the indole ring of compound 4 were observed as singlet at δ 3.39 and 2.55 ppm, respectively (Figure 5).

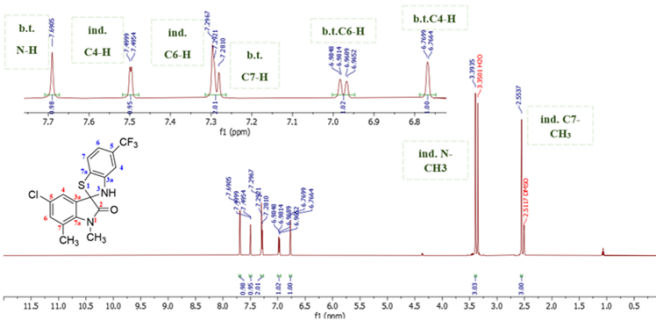

Figure 5. ^{1}H NMR (600 MHz, DMSO-d_6) spectrum of compound **4** (δ 0-12 ppm).

In the ^{13}C NMR-APT spectrum of compound **4**, signals (OCF_3, benzothiazoline C_5, C_6, and C_4) that showed the ^{13}C-^{19}F coupling were displayed as a quartet. These signals resonated at δ 124.94, 127.22, 116.01 and 104.21 ppm, respectively. The C_{3_a} signal, which resonates at the lowest field among the benzothiazoline carbons, was detected at δ 147.94 ppm, while the benzothiazoline C_{7_a} signal was seen at δ 129.98 ppm. The 2-indolinone C=O (δ 175.02 ppm), C_{7_a} (δ 139.93 ppm), C_6 (δ 134.00 ppm), C_{3_a} (δ 131.90 ppm), C_5 (δ 127.33 ppm), C_4 (δ 123.58 ppm), and C_7 (δ 123.42 ppm) signals were determined. Methyl protons at positions 1- and 7- of the indole ring of compound 4 showed at δ 29.81 and 18.44 ppm, respectively (Figure 6). The selected ^1H and ^{13}C NMR-APT chemical shift values (ppm) of compound **4** are shown in Figure 7.

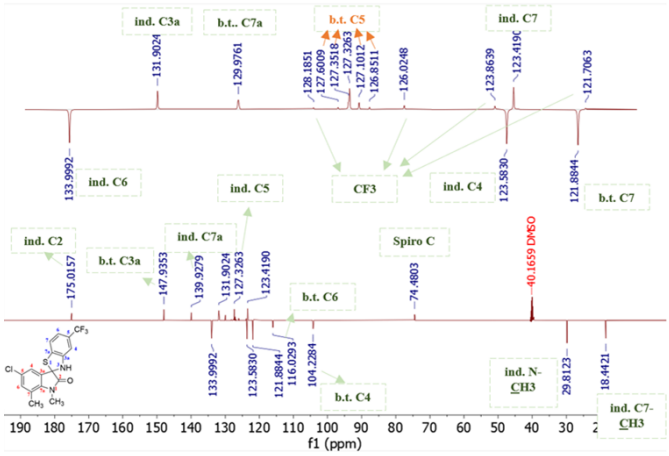

Figure 6. ^{13}C NMR-APT (126 MHz, DMSO-d_6) spectrum of compound **4** (δ 0-210 ppm).

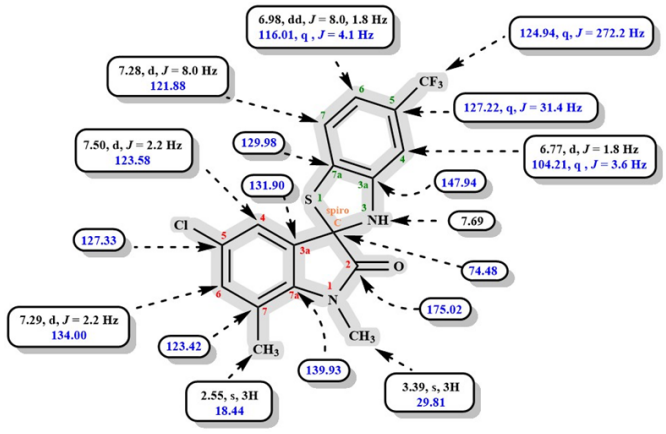

Figure 7. Selected ^1H and ^{13}C NMR-APT chemical shift values (ppm) of compound **4.**

Further verification was obtained from the HSQC-2D spectra of compound **4**, which clearly show the ^1H–^{13}C connections and allow definite assignment of the ^1H and ^{13}C resonances (Figure 8). The presence of spiro C (δ 74.48 ppm) in the ^{13}C NMR-APT and HMBC-2D spectra is evidence of a spirocyclic structure. These data are consistent with spiroindolinone studies in the literature (Figures 6 and 9) (Dandia et al., 1990; Dandia et al., 2004; Ermut et al., 2014; Karalı et al., 2010; Naumov & Anastasova, 2001).

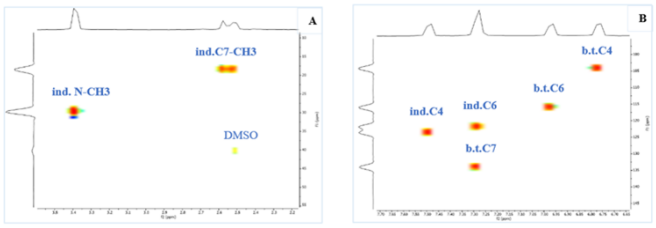

Figure 8. HSQC-2D (600 MHz, DMSO-d_6) spectra of compound **4** (**A**. δ 10-55 ppm; **B.** δ 90-150 ppm).

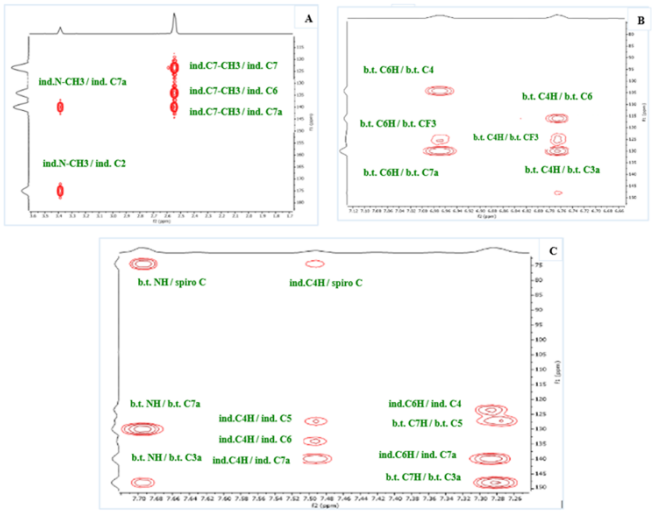

Figure 9. HMBC-2D (600 MHz, DMSO-d_6) spectra of compound **4** (**A**. δ 1.7-3.6 ppm; B. δ 6.65 – 7.12 ppm; C. δ 7.26-7.70 ppm).

When the HMBC-2D spectrum of compound **4** was examined, the interaction of the indole N-CH_3 protons with the indole C_{7_a} and C_2 carbons and the interaction of the indole C_7-CH_3 protons with the indole C_7, C_6 and C_{7_a} carbons were observed (Figure 9A). The benzothiazoline C_6 proton interacted with the benzothiazoline C_4, CF_3, and C_{7_a} carbons and the C_4 proton of benzothiazoline interacted with the benzothiazoline C_6, CF_3, and C_{3_a} carbons. (Figure 9B). The interaction of the spiro C signal with the benzothiazoline NH and indole C_4 proton signals supports the accuracy of the spiroindolinone structure. Furthermore, benzothiazoline NH interacted with benzothiazoline C_{7_a} and C_{3a} carbons, while the indole C_4 proton interacted with indole C_5, C_6, and C_{7_a} carbons. Additionally, it was determined that the indole C_6 proton interacted with the indole C_4 and C_{7_a} carbons, while the benzothiazoline C_7 proton interacted with the benzothiazoline C_5 and C_{3_a} carbons (Figure 9C).

In the LC-MS spectrum of compound **4** taken by positive ionization technique, the base peak was $[M+Na]^+$ (m/z 407.0) ion, and $[M+H]^+$ (m/z 385.0) peak was confirmed its molecular weight. Additionally, $[M+Na]^+$+2 and $[M+H]^+$+2 peaks resulting from ^{35}Cl and ^{37}Cl isotopes of the chlorine atom at the position 5- of the 2-indolinone ring were also observed in the spectrum at relative abundance ratios of 100:38 and 38:13, respectively.

X-ray single-crystal diffraction analysis

ORTEP 3 (Farrugia, 1997) drawing with atom numbering obtained by X-ray analysis of compound **4** confirms its molecular structure and atom connectivity, as depicted in Figure 10. Compound **4** consists of an indole ring [N1/C3-C10] and benzothiazole [S1/N2/C11-C16] ring connected to the trifluoromethyl group. The atoms O1 and C/1 are positioned at distances of -0.0683(16) and 0.0984(7) Å, respectively from the least square plane defined by all the atoms of the indole ring. In the molecule, the indole ring system is planar, with minimal deviations from the mean plane: -0.0269 Å for the C7 and 0.0259 Å for the C5 atoms, respectively. However, the indolinone group is not planar, and the O1 atom deviates from planarity by -0.068(2) Å. The benzothiazole ring exhibited non-planar characteristics, with the C10 atom deviating from the mean plane of S1/C12/C11/N2 by 0.518(2) Å. The indole ring system [N1/C3-C10] is at a dihedral angle of 89.48(5)° relative to the mean plane of the S1/N2/C11-C16 moiety, suggesting a near-perpendicular orientation between the indole ring [N1/C3-C10] and the benzothiazole ring system.

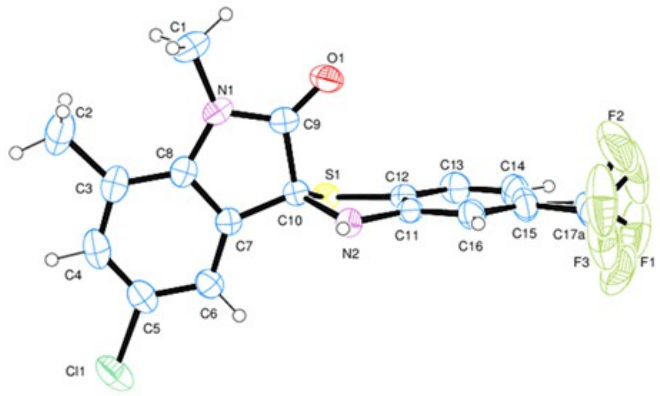

Figure 10. HMBC-2D (600 MHz, DMSO-d_6) spectra of compound **4** (View of compound **4** with the atom numbering scheme. Displacement ellipsoids for non-H atoms are drawn at the 30% probability level.

The structure exhibited disorder in the trifluoromethyl group connected to C17, with occupancy factors of 0.61(2) for component one and 0.39(2) for component a. The C17 and F atoms were found at two distinct positions, constrained by the SAME restriction. Despite this separation into two positions, the CF_3 group demonstrates continuous positional disorder, as evidenced by the significant thermal vibration parameters. The C17-F_3 bond lengths vary notably, ranging from 1.259 to 1.325 Å for one disordered component and from 1.260 to 1.315 Å for component a.

The crystal structure of compound **4** is stabilized by both intra- and intermolecular hydrogen bonds. The O1 atom within the indolinone moiety forms an intra-molecular hydrogen bond interaction [C1···O1 2.842(3) Å, C1-H1B 0.96(3) Å, and C1-H1B···O1 104.7(2)°]. The intermolecular hydrogen bond of N···O type between adjacent molecules is oriented along the c axis [N2···O1i 3.172(2) Å, N2-H2 0.81(2) Å, and N2-H2···O1i 150(2)° with symmetry code: (i) x, 1/2-y, 1/2+z]. Figures 11 and 12 show the intermolecular N-H···O hydrogen bonding interactions along the c axis, and Figure 12a shows the layers of molecules that are parallel to the (010) plane. A view of the crystal packing and hydrogen bonding of compound **4** along the a axis (a), b axis (b), and c axis (c) is provided in Figure 12a-c.

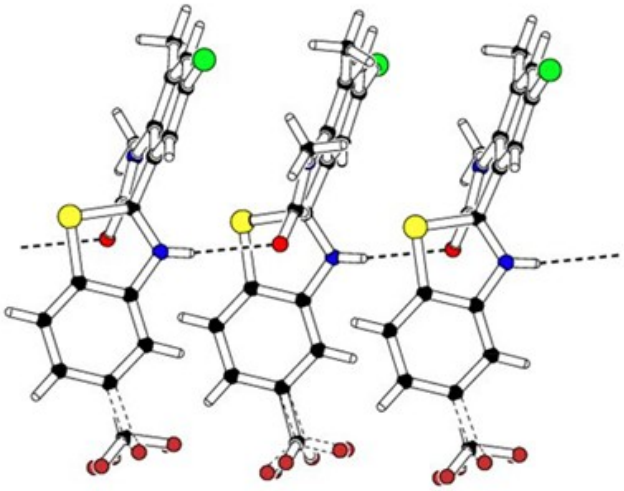

Figure 11. A view of N-H···O hydrogen bonding interactions of compound **4.**

All bond lengths and angles were within normal ranges and matched those documented in prior studies (Karalı et al., 2010; Akkurt et al. 2010). The torsion angle N1-C9-C10-N2 is measured at -132.3(2)°, indicating an -anti-clinal (-ac) conformation, while the C7–C10–N2–C11 torsion angle measures 156.9(2)°, indicating an antiperiplanar (ap) conformation. Details of the data collection conditions and the parameters of the refinement process are given in Table 1. The selected bond lengths and angles are presented in Table 2.

In silico analyzes

A factor considered for the synthesised compounds to be potential drug candidates is whether they have drug-like proper-

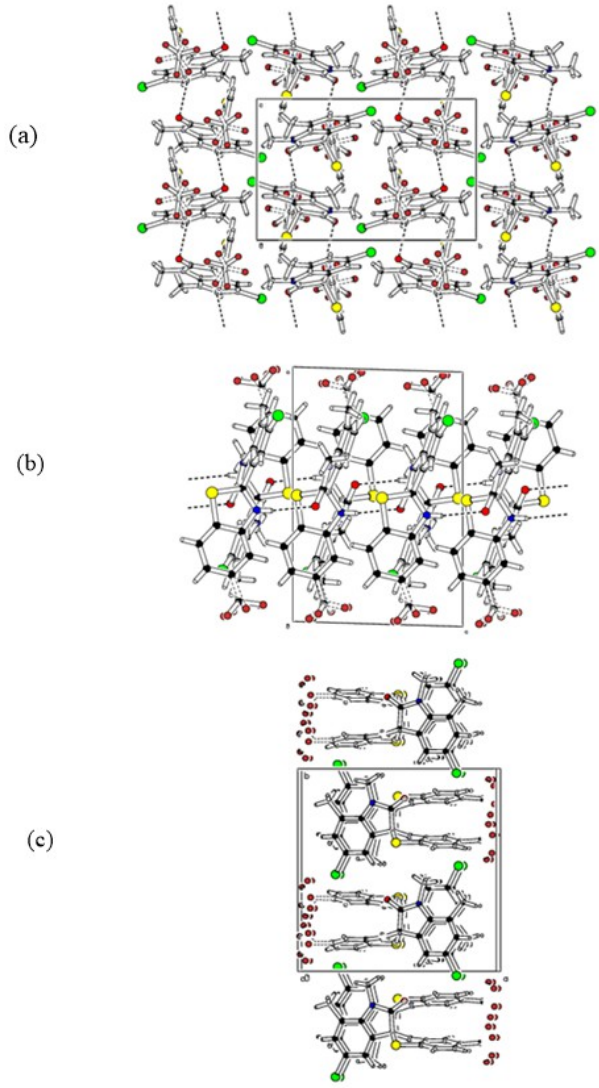

Figure 12. A view along the a axis (a), b axis (b), c axis (c) of the crystal packing and hydrogen bonding of compound **4.**

Table 1. Crystal data and structure refinement parameters for compound **4.**

Crystal data	
Chemical formula	$C_{17}H_{12}C/F_3N_2OS$
Formula weight	384.80
Crystal system, Space group	Monoclinic, $P2_1/c$
Temperature (K)	293(2)
***a*, *b*, *c* (Å)**	13.667(3), 14.063(2), 9.1013(19)
***β* (°)**	91.742 (17)
***V* (Å^3)**	1748.4 (6)
Z	4
Radiation type	Mo Kα
***μ* (mm^{-1})**	0.375
Crystal size (mm)	0.790 × 0.503 × 0.260
Data collection	
Diffractometer	STOE IPDS 2
Absorption correction	Integration
T_{min}, T_{max}	0.758, 0.906
No. of measured, independent and observed [I > 2σ(I)] reflections	13628, 3894, 2608
Rint	0.0731
(sin θ/λ)max (Å^{-1})	0.646
Refinement	
R[F^2 > 2σ(F^2)], wR(F^2), GOF	0.0427, 0.0930, 0.965
No. of reflections	3894
No. of parameters	269
No. of restraints	10
H-atom treatment	H atoms treated by a mixture of independent and constrained refinement
$\Delta\rho_{max}$, $\Delta\rho_{min}$ (e Å^{-3})	0.285, −0.324

Table 2. Selected bond lengths and angles of compound **4.**

Bond lengths (Å)			
S1–C10	1.8508(18)	C7–C8	1.395(3)
S1–C12	1.767(2)	N1–C8	1.423(3)
C11–C12	1.412(3)	N1–C9	1.361(3)
N2–C11	1.393(2)	N1–C1	1.457(3)
N2–C10	1.448(3)	O1–C9	1.221(2)
C10–C9	1.546(3)	C*l*1–C5	1.742(2)
C7–C10	1.507(3)	N2–H2	0.81(2)
Bond angles (°)			
C12–S1–C10	90.00(8)	O1–C9–N1	126.59(18)
N2–C10–S1	103.29(12)	O1–C9–C10	125.28(18)
C11–N2–C10	113.09(15)	C9–N1-C8	111.19(15)
O1–C9–C10	125.28(18)	C9–N1–C1	120.34(18)
N1–C9–C10	108.12(16)	C4–C5–C*l*1	119.03(18)
C4–C3–C2	119.2(2)	C6–C5–C*l*1	119.82(19)

ties. Lipinski's RO5 has traditionally been used for many years to evaluate the oral bioavailability and drug-like properties of compounds (Lipinski, Lombardo, Dominy & Feeney, 1997). According to Lipinski's RO5, a candidate molecule must fulfil these criteria in order to be orally usable and to have drug-like properties, and it is expected that at most one rule is not complied with. To evaluate the suitability of compound **4** to Lipinski's RO5, a comprehensive *in silico* study was performed using the Qikprop module (Schrödinger, LLC, New York, NY 2018), focusing on various physicochemical parameters.

To evaluate the suitability of compound **4** to Lipinski's RO5, a comprehensive *in silico* investigation was carried out using the Qikprop module (Schrödinger, LLC, New York, NY 2018), focusing on various physicochemical parameters and ADME criteria. The calculation of the molecular weight of compound **4** as 384.80 and logP value as 3.88 shows compliance with the criteria. In addition, it is predicted that compound **4** will have high biological activity with the determination of hydrogen bond donor and acceptor numbers as 1.0 and 4.5, respectively, which is a measure of its capacity to interact with target systems. With zero violations of the Lipinski's RO5, compound **4** demonstrated potential as a drug candidate (Table 3).

The water solubility of compounds is expressed by the "LogS" value and is extremely important for the oral absorption capacity of the drug (Di, Fish & Mano, 2012). When the logS value, which should be in the range of (-6.5)-0.5, was examined, this value was calculated as -4.902 for compound **4**. LogBB defines the blood-brain barrier partition coefficient and CNS defines the central nervous system activity. The CNS value should be in the range of (-2)-2 and LogBB value should be in the range of (-3)-1.2. The CNS activity of the compound whose LogBB value is close to negative values and CNS value

Table 3. Compatibility of compound **4** with Lipinski's RO5.

Molecular weight	QPlogP octanol/water	Number of hydrogen bond donors	Number of hydrogen bond acceptors	Number of RO5 not complied with
Ref. <500	**<5**	**<5**	**<10**	**≤1**
384.80	3.88	1	4.5	0

Table 4. Compatibility of compound **4** with some physicochemical parameters and ADME criteria.

QLogS [a]	QLogBB [b]	CNS [c]	QLogKhsa [d]	PMDCK [e]	Rot [f]	HOA(%) [g]
Ref. (-6.5)-0.5	**(-3)-1.2**	**(-2)-2**	**(-1.5)-1.5**	**<25 poor >500 very good**	**≤3**	**>80 high activity <25 weak activity**
-4.902	0.977	-2	0.509	6212.441	0	100

[a] Solubility in water
[b] Blood-brain barrier permeation capacity
[c] Central nervous system activity
[d] Binding rate to human serum albümin
[e] MDCK cell permeability
[f] Number of rotatable bonds
[g] Percentage of human oral absorption

is close to -2 decreases, thus it has difficulty in crossing the blood-brain barrier. The LogBB value of compound **4** was calculated as 0.977 and the CNS value as -2. This may help to reduce side effects and is important for the safety of the candidate compound. The logKhsa value, which describes the binding rate to human serum albumin, should be between (-1.5) and (1.5). This value was measured as 0.509 and fulfilled these criteria. Madin-Darby Canine Kidney (MDCK) cell permeability (PMDCK) helps assess the ability of a compound to pass through the cell membrane, aiding in determining the drug's bioavailability and efficacy. If this value is less than 25, it indicates poor cell permeability, while more than 500 signifies excellent cell permeability. For compound **4**, this value was calculated as 6212.441. The number of rotatable bonds (Rot) of compound **4** was determined to be zero. This indicates that the molecule is in a rigid structure. The percentage of oral absorption in men (HOA) was defined as > 80 for high oral activity and < 25 for poor oral activity. The calculation of this value as 100 for compound **4** indicates that the compound **4** has high oral absorption (Table 4).

CONCLUSION

The new 5'-chloro-1',7'-dimethyl-5-(trifluoromethyl)-3*H*-spiro[1,3-benzothiazole-2,3'-indol]-2'-on (**4**) was synthesized in good yield. The molecular, spirocyclic and stereoisomeric structure of the compound **4** was determined by spectral and X-ray single crystal diffraction analyses. In the crystal, both intra- and intermolecular hydrogen bonds stabilize the molecular packing. The intermolecular N-H···O hydrogen bonding interactions reveal layers of molecules that are parallel to the (010) plane. Additionally, in silico analyses showed that compound **4** has the appropriate biochemical properties for the desired pharmacokinetics and reduced toxicity in terms of drug-ability criteria.

Supplementary material

CCDC-2335656 contains the supplementary crystallographic data for the compound reported in this paper. These data can be obtained free of charge at www.ccdc.cam.ac.uk/conts/ retrieving.html [or from the Cambridge Crystallographic Data Centre (CCDC), 12 Union Road, Cambridge CB2 1EZ, UK; fax: +44(0)1223 336033; e-mail: deposit@ccdc.cam.ac.uk]. Supplementary data associated with this article can be found in the online version at http://dx.doi.org/10.1016/j.saa.2013.08.054.

Peer-review: Externally peer-reviewed.

Author Contributions: Conception/Design of Study- N.K., A.B.T.; Data Acquisition- A.B.T.; Data Analysis/Interpretation- N.K., F.B.K., A.B.T.; Drafting Manuscript- A.B.T, N.K., F.B.K.; Critical Revision of Manuscript- N.K., F.B.K.; Final Approval and Accountability- N.K., F.B.K., A.B.T.

Conflict of Interest: The authors have no conflict of interest to declare.

Financial Disclosure: This work was supported by The Scientific Research Projects Coordination Unit of Istanbul University (TSA-2020-37008).

Acknowledgement: We would like to thank Prof. Dr. Ömer Andaç for his contribution to X-ray single crystal diffraction analysis studies. Asu Büşra TEMIZER who is the author of this study is supported by Council of Higher Education (100/2000 YOK doctoral scholarships) and The Scientific and Technological Research Council of Türkiye (TUBITAK-BIDEB 2211/A National PhD Scholarship Program).

ORCID IDs of the authors

Asu Busra Temizer 0000-0003-1811-093X
Filiz Betül Kaynak 0000-0002-3216-4021
Nilgun Karalı 0000-0002-6916-122X

REFERENCES

Abdelmouna, K., Laghchioua, F., Paz, F. A., Mendes, R. F., Moura, N. M., Faustino, M. A., . . . & Neves, M. G. (2023). Development of catalyst-free approach to synthesize novel spiro[indoline-3,1-pyrazolo[1,2-a]pyrazoles] via 1,3-dipolar cycloaddition. *Journal of Molecular Structure, 1272*, 134170.

Akdemir, Ö. G., & Ermut, N. K. G. (2013). Antimicrobial and antiviral activity of spiroindolinones bearing benzothiazole moiety. *Journal of Faculty of Pharmacy of Istanbul University, 43*(1), 1-11.

Akkurt, M., Karaca, S., Ermut, G., Karalı, N., & Büyükgüngör, O. (2010). 5-Chlorobenzothiazole-2-spiro-3-indolin-2-one. *Acta Crystallographica Section E: Structure Reports Online, 66*(2), 399-400.

Allam, Y. A., & Nawwar, G. A. (2002). Facile synthesis of 3-spiroindolines. *Heteroatom Chemistry: An International Journal of Main Group Elements, 13*(3), 207-210.

Altowyan, M. S., Soliman, S. M., Haukka, M., Al-Shaalan, N. H., Alkharboush, A. A., & Barakat, A. (2022). Synthesis, characterization, and cytotoxicity of new spirooxindoles engrafted furan structural motif as a potential anticancer agent. *ACS Omega, 7*(40), 35743-35754.

Baeyer, A. (1900). Systematik und nomenclatur bicyclischer kohlenwasserstoffe. *Berichte der Deutschen Chemischen Gesellschaft, 33*(3), 3771-3775.

Bariwal, J., Voskressensky, L. G., & Van der Eycken, E. V. (2018). Recent advances in spirocyclization of indole derivatives. *Chemical Society Reviews, 47*(11), 3831-3848.

Castineiras, A., Gómez, M., & Sevillano, P. (2000). 2-(2,3-Dihydro-1,3-benzothiazol-2-yl)phenyl(diphenyl)phosphine oxide. Synthesis and characterization by IR and NMR spectroscopy and X-ray diffractometry. *Journal of Molecular Structure, 554*(2-3), 301-306.

Dandia A., Khanna S., & Joshi K C. (1990). Reactions of fluorinated isatin derivatives with 2-aminothiophenol. *Journal Indian Chemistry Society, 67*, 824-826.

Dandia, A., Singh, R., & Arya, K. (2004). Microwave induced dry-media synthesis of spiro[indole-thiazolidinones/thiazinones] as potential antifungal and antitubercular agents and study of their reactions. *Phosphorus, Sulfur, and Silicon, 179*(3), 551-564.

Dandia, A., Singh, R., Khaturia, S., Mérienne, C., Morgant, G., & Loupy, A. (2006). Efficient microwave enhanced regioselective synthesis of a series of benzimidazolyl/triazolyl spiro[indole-thiazolidinones] as potent antifungal agents and crystal structure of spiro[3*H*-indole-3,2-thiazolidine]-3(1,2,4-triazol-3-yl)-2,4(1*H*)-dione. *Bioorganic & Medicinal Chemistry, 14*(7), 2409-2417.

Di, L., Fish, P. V., & Mano, T. (2012). Bridging solubility between drug discovery and development. *Drug Discovery Today, 17*(9-10), 486-495.

Ding, A., Meazza, M., Guo, H., Yang, J. W., & Rios, R. (2018). New development in the enantioselective synthesis of spiro compounds. *Chemical Society Reviews, 47*(15), 5946-5996.

Dowlatabadi, R., Khalaj, A., Rahimian, S., Montazeri, M., Amini, M., Shahverdi, A., & Mahjub, E. (2011). Impact of substituents on the isatin ring on the reaction between isatins with orthophenylenediamine. *Synthetic Communications, 41*(11), 1650-1658.

Ermut, G., Karalı, N., Özsoy, N., & Can, A. (2014). New spiroindolinones bearing 5-chlorobenzothiazole moiety. *Journal of Enzyme Inhibition and Medicinal Chemistry, 29*(4), 457-468.

Farrugia, L. J. (1999). WinGX suite for small-molecule single-crystal crystallography. *Journal of Applied Crystallography, 32*, 837-838.

Farrugia, L. J. (1997). ORTEP-3 for Windows-a version of ORTEP-III with a Graphical User Interface (GUI). *Journal of Applied Crystallography*, 30, 565.

Jain, R., Sharma, K., & Kumar, D. (2012). A greener, facile and scalable synthesis of indole derivatives in water: reactions of indole-2,3-diones with 1,2-difunctionalized benzene. *Tetrahedron Letters, 53*(46), 6236-6240.

Jiang, T., Kuhen, K. L., Wolff, K., Yin, H., Bieza, K., Caldwell, J., . . . He, Y. (2006). Design, synthesis and biological evaluations of novel oxindoles as HIV-1 non-nucleoside reverse transcriptase inhibitors. Part I. *Bioorganic & Medicinal Chemistry Letters, 16*(8), 2105-2108.

Joshi K.C., Dandia A., & Khanna S. (1990). Studies in spiroheterocycles: Part XXIII-Investigation on the reactions of indole-2,3-diones with 2-aminothiophenol and 2-aminophenol. *Indian Journal Chemistry Sect B: Organic Chemistry Include Medicinal Chemistry, 29B*: 824-829.

Karalı, N., Güzel, Ö., Özsoy, N., Özbey, S., & Salman, A. (2010). Synthesis of new spiroindolinones incorporating a benzothiazole moiety as antioxidant agents. *European Journal of Medicinal Chemistry, 45*(3), 1068-1077.

Laatsch, H., Thomson, R. H., & Cox, P. J. (1984). Spectroscopic properties of violacein and related compounds: crystal structure of tetramethylviolacein. *Journal of the Chemical Society, Perkin Transactions 2*(8), 1331-1339.

Lipinski, C. A., Lombardo, F., Dominy, B. W., & Feeney, P. J. (1997). Experimental and computational approaches to estimate solubility and permeability in drug discovery and development settings. *Advanced Drug Delivery Reviews, 23*(1-3), 3-25.

Murugan, R., Anbazhagan, S., & Narayanan, S. S. (2009). Synthesis and in vivo antidiabetic activity of novel dispiropyrrolidines through [3+2]cycloaddition reactions with thiazolidinedione and rhodanine derivatives. *European Journal of Medicinal Chemistry, 44*(8), 3272-3279.

Nardelli, M. (1995). PARST: a system of Fortran routines for calculating molecular structure parameters from the results of crystal structure analyses. *Journal of Applied Crystallography, 28*, 659.

Naumov, P., & Anastasova, F. (2001). Experimental and theoretical vibrational study of isatin, its 5-(NO_2, F, Cl, Br, I, CH_3) analogues and the isatinato anion. *Spectrochimica Acta Part A: Molecular and Biomolecular Spectroscopy, 57*(3), 469-481.

Popp, F. D. (1969). The reaction of Isatin with aromatic-o-diamines. *Journal of Heterocyclic Chemistry, 6*(1), 125-127.

Rottmann, M., McNamara, C., Yeung, B. K. S., Lee, M. C. S., Zou, B., Russell, B., . . . Diagana, T. (2010). Spiroindolones, a potent compound class for the treatment of malaria. *Science, 329*(5996), 1175-1180.

Santes, V., Rojas-Lima, S., Santillan, R. L., & Farfán, N. (1999). Synthesis and study of isomeric benzo[1,4]oxazines and benzothiazolines by NMR spectroscopy and X-ray crystallography. *Monatshefte für Chemie, 130*(12), 1481-1486.

Schwertz, G., Witschel, M. C., Rottmann, M., Leartsakulpanich, U., Chitnumsub, P., Jaruwat, A., ... Diederich, F. (2018). Potent inhibitors of plasmodial serine hydroxymethyltransferase (SHMT) featuring a spirocyclic scaffold. *ChemMedChem*, 13(9), 931-943.

SDBS. https://sdbs.db.aist.go.jp/sdbs/cgi-bin/landingpage?sdbsno=3865.

Shangary, S., Qin, D., McEachern, D., Liu, M., Miller, R. S., Qiu, S., ... Wang, S. (2008). Temporal activation of p53 by a specific MDM2 inhibitor is selectively toxic to tumors and leads to complete tumor growth inhibition. *Proceedings of the National Academy of Sciences, 105*(10), 3933-3938.

Sheldrick, G. M. (1997). SHELXS-97, Program for the Solution of Crystal Structures, University of Gottingen, Germany.

Sheldrick, G. M. (2015). SHELXL-2014, Crystal Structure Refinement with SHELXL. *Acta Crystallographica Section* C, 71, 3-8.

Spek, A. L. (2009). Structure validation in chemical crystallography, *Acta Crystallographica Section D Structural Biology*, D65, 148-155.

Stoe & Cie, (2002). X-AREA (Version 1.18) X-RED32 (Version 1.04) Stoe & Cie. Darmstadt, Germany.

Zhao, Y., Yu, S., Sun, W., Liu, L., Lu, J., McEachern, D., ... Wang, S. (2013). A potent small-molecule inhibitor of the MDM2–p53 interaction (MI-888) achieved complete and durable tumor regression in mice. *Journal of Medicinal Chemistry, 56*(13), 5553-5561.

How cite this article

Temizer, A.B., Kaynak, F.B., & Karalı, N. (2024). Synthesis, characterization, and crystal structure of a novel spirocyclic 2-indolinone bearing a 5-(trifluoromethyl)benzothiazoline moiety. *İstanbul Journal of Pharmacy, 54*(3): 456–465. DOI: 10.26650/IstanbulJPharm.2024.1449135